

# Flammability and Mechanical Properties of Wood Flour-Filled Polypropylene Composites

M. B. Abu Bakar,<sup>1</sup> Z. A. Mohd Ishak,<sup>1</sup> R. Mat Taib,<sup>1</sup> H. D. Rozman,<sup>2</sup> S. Mohamad Jani<sup>3</sup>

<sup>1</sup>School of Materials and Mineral Resources Engineering, Engineering Campus, Universiti Sains Malaysia, 14300 Nibong Tebal, Seberang Perai Selatan, Penang, Malaysia

<sup>2</sup>School of Industrial Technology, Universiti Sains Malaysia, 11800 Minden, Penang, Malaysia

<sup>3</sup>Wood Composite Unit, Forest Research Institute Malaysia, 52109 Kepong, Selangor, Malaysia

Received 29 January 2009; accepted 17 November 2009

DOI 10.1002/app.31791

Published online 27 January 2010 in Wiley InterScience (www.interscience.wiley.com).

**ABSTRACT:** Polypropylene (PP) composites filled with wood flour (WF) were prepared with a twin-screw extruder and an injection-molding machine. Three types of ecologically friendly flame retardants (FRs) based on ammonium polyphosphate were used to improve the FR properties of the composites. The flame retardancy of the PP/WF composites was characterized with thermogravimetric analysis (TGA), vertical burn testing (UL94-V), and limiting oxygen index (LOI) measurements. The TGA data showed that all three types of FRs could enhance the thermal stability of the PP/WF/FR systems at high temperatures and effectively increase the char residue formation. The FRs could effectively reduce the flammability of the PP/WF/FR composites by achieving V-0 UL94-V classification. The increased LOI also showed that the flammability of the PP/WF/FR composites was reduced with the

addition of FRs. The mechanical property study revealed that, with the incorporation of FRs, the tensile strength and flexural strength were decreased, but the tensile and flexural moduli were increased in all cases. The presence of maleic anhydride grafted polypropylene (MAPP) resulted in an improvement of the filler–matrix bonding between the WF/intumescent FR and PP, and this consequently enhanced the overall mechanical properties of the composites. Morphological studies carried out with scanning electron microscopy revealed clear evidence that the adhesion at the interfacial region was enhanced with the addition of MAPP to the PP/WF/FR composites. © 2010 Wiley Periodicals, Inc. *J Appl Polym Sci* 116: 2714–2722, 2010

**Key words:** composites; flame retardance; mechanical properties; poly(propylene); (PP)

## INTRODUCTION

During the past decade, the acceptance of wood-derived fillers in the plastic industry has been growing because of their high specific properties, biodegradability, renewability, and low cost. These are combined with satisfactory processing characteristics, that is, the ability to use extrusion, compression, and injection moldings, as well as less abrasion of processing machinery. These facts, as well as lower costs in comparison with other inorganic fillers and fibers, promise a bright future for the utilization of wood-derived fillers in the plastic industry. The thermoplastics that are commonly used in combination with such materials to produce wood–plastic composites (WPCs) are polypropylene (PP) and polyethylene. WPCs have been marketed for furniture, building components such as flooring and sid-

ing, and outdoor products such as benches, decking, and fencing.

As organic materials, polymers and wood-derived fillers such as wood flour (WF) are very sensitive to flame. Thus, the improvement of the flame retardancy of composite materials has become important for complying with the safety requirements of WPC products. The most expeditious method used to acquire flame retardancy is the incorporation of flame retardants (FRs) that can interfere with combustion at a particular stage of the process so that the resulting system shows satisfactory flame retardancy.<sup>1</sup> The most widely used additive-type FRs are inorganic, halogenated, and phosphorous compounds such as ammonium polyphosphate (APP), hexabromocyclododecane (HBCD), magnesium hydroxide [Mg(OH)<sub>2</sub>], and aluminum hydroxide [Al(OH)<sub>3</sub>].<sup>1–3</sup>

In recent years, intumescent flame retardant (IFR) additives have been increasingly used to retard the flammability of polymers such as PP. Compared to halogen-containing compounds, IFR additives generate little smoke, no corrosive gas, and no flame dripping and are nontoxic.<sup>3–6</sup> An IFR additive is actually a system that consists of an acid source, a blowing agent, and a carbonific agent or char. During combustion, the chemical and physical reactions of these

Correspondence to: Z. A. M. Ishak (zarifin@eng.usm.my).

Contract grant sponsor: Malaysian Ministry of Science, Technology, and Innovation (through a Prioritized Research/Intensification of Research in Priority Areas grant); contract grant number: 304/PBAHAN/6050054.

TABLE I  
Commercial FRs

FR code	FR grade/trade name	Density (g/cm <sup>3</sup> )	Main constituent material	P <sub>2</sub> O <sub>5</sub> content (%)	Solubility in water (g/100 mL)	pH	D <sub>50</sub> (μm)	Additional information
APP1	Cros 484	1.91	APP	72	0.5	5–6	18	—
APP2	Cros 486	1.97	APP	71	0.1	6–7	18	Silane surface treatment
IFR	Budit 3157	1.80	APP	48	2.0	7	18	Intumescent grade

constituents form rigid, voluminous foamed residue or char, which offers protection to the underlying substrate from further decomposition and offsets the melt-dripping tendency as well.<sup>7</sup> In traditional IFR systems, APP has been used as the acid source, melamine has been used as the blowing agent, and pentaerythritol has been used as the carbonific agent.<sup>3</sup>

One of the major drawbacks facing the production of WPCs is the poor interfacial compatibility between the filler and the polymer matrices.<sup>3</sup> A WPC is composed of a blend of hydrophobic plastics, such as polyethylene and PP, and hydrophilic wood-derived fillers. To improve the interfacial properties of the blend, a compatibilizer or a coupling agent is generally used. Compatibilizers or coupling agents contain both a polar functional group that can interact or react with the hydroxyl groups of the wood-derived fillers and a nonpolar entity that is more compatible with the hydrocarbon polyolefin chains of the polyolefin.<sup>8</sup> Maleic anhydride grafted polymers, such as maleated polyethylene and maleated polypropylene (MAPP), are widely used as compatibilizers for improving the mechanical properties of WPCs.<sup>3</sup>

Previously, many studies of the flammability of polymers have been reported in the literature.<sup>1–10</sup> However, there appears to be limited work published on the application of different types of FRs in WPCs. For example, Li and He<sup>3</sup> reported the use of single APPs and IFRs in linear low-density polyethylene/WF composites. Le Bras and co-workers<sup>9</sup> used the APP/pentaerythritol/melamine system in PP/flax blends as an intumescent model additive to obtain an optimized FR formulation. The aim of this study was to investigate and compare the fire retardancy of PP/WF composites containing various commercially available FRs such as APP and intumescent ready-to-use products based on APP. In addition, the effect of MAPP on achieving a balance of mechanical and FR properties in PP/WF composites was also investigated.

## EXPERIMENTAL

### Materials

Copolymer-grade PP (Pro-Fax SM240) with a melt flow index (MFI) of 25 g/10 min (at 230°C and 2.16 kg) and a density of 0.894 g/cm<sup>3</sup> was supplied by

Titan Petchem (M) Sdn. Bhd. (Johor, Malaysia). Light red meranti (*Shorea* spp.) WF with a 35-mesh size [mean particle size ( $D_{50}$ ) = 503.95 μm] and a density of 1.294 g/cm<sup>3</sup> was obtained from the Forest Research Institute of Malaysia (Selangor, Malaysia). The MAPP compatibilizer (Polybond 3200 with 1.0 wt % maleic anhydride) was purchased from Uniroyal-Crompton (Middlebury, CT). Commercially available FR additives purchased from Budenheim Iberica (La Zaida, Spain) are listed in Table I.

### Sample preparation

Table II lists the sample formulations for PP and its composites. All WPC formulations were compounded in a Sino PSM30 co-rotating, open-vent, twin-screw extruder (Sino-Alloy Machinery Inc., Taipei Hsien, Taiwan) with a length/diameter ratio of 40 at 180°C and 150 rpm and were subsequently pelletized. The pellets were dried overnight at 75°C and then injected with a Haitian HTF160X 60-ton injection molding machine (Ningbo Haitian Heavy Work Machinery Co., Ltd., Ningbo, China) into molds to produce the test specimens for flammability and mechanical tests. A nozzle temperature of 195°C and an injection pressure of 55 bar were employed.

### Sample characterization

#### MFI

MFI values were determined with a Dynisco polymer test (Alpha Technologies, Inc., USA) according to ASTM D 1238 with a load of 2.16 kg at 190°C (instead of the 230°C typically used for PP) to preserve the WF from thermal degradation. The

TABLE II  
Sample Formulations of PP and Its Composites

Sample code	Composition (%)					
	PP	WF	APP1	APP2	IFR	MAPP <sup>a</sup>
PP0	100	—	—	—	—	—
PP1	40	60	—	—	—	—
PP2	40	30	30	—	—	—
PP3	40	30	—	30	—	—
PP4	40	30	—	—	30	—
PP5	40	30	—	—	30	5

<sup>a</sup> This accounted for 5% of the weight percentage of the filler.

**TABLE III**  
**MFI of PP and Its Composites**

Sample code	MFI (g/10 min)
PP0	10.40 ± 0.11
PP1	2.44 ± 0.27
PP2	0.20 ± 0.01
PP3	0.21 ± 0.02
PP4	0.47 ± 0.06
PP5	1.11 ± 0.04

capillary diameter was 2.096 mm. Each sample was tested five times, and the results were averaged.

#### Thermogravimetric analysis (TGA)

The TGA study was carried out on a PerkinElmer Pyris 6 thermal analyzer (Waltham, MA) at a constant heating rate of 20°C/min under a pure nitrogen flow at 20 mL/min. The temperature ranged from the ambient temperature to 800°C. The weight of each sample was kept within 3–5 mg.

#### Flammability properties

The flame retardancy of all samples was characterized by vertical burn test (UL94-V) and limiting oxygen index (LOI) methods according to ASTM D 3801 and ASTM D 2863, respectively. The UL94-V of all samples was measured on an HVUL horizontal vertical flame chamber instrument produced by Atlas Materials Testing Technology (Chicago, IL). Rectangular specimens with dimensions of 127 × 12.7 × 3.2 mm<sup>3</sup> were used in this test.

The LOI of all samples was tested on an oxygen index instrument at room temperature. In this test, a sample is suspended vertically inside a closed chamber (usually a glass or clear plastic enclosure). The chamber is equipped with oxygen and nitrogen gas inlets so that the atmosphere in the chamber can be controlled. The sample is ignited from the bottom, and the atmosphere is adjusted to determine the minimum amount of oxygen needed to just sustain burning. This minimum oxygen content, expressed as a percentage of the oxygen/nitrogen atmosphere, is called the oxygen index.

#### Mechanical properties

Tensile and flexural tests were conducted at room temperature (23°C) with an Instron model 3366 universal mechanical testing machine (Instron, Canton, MA) with a load capacity of 10 kN. The tensile test was conducted in accordance with ASTM D 638 with type 1 test specimen dimensions at a crosshead speed of 5 mm/min. The tensile modulus, tensile strength, and elongation at break were measured. The flexural test with specimen dimensions of 127 × 12.7 × 3.2 mm<sup>3</sup> was conducted in accordance with ASTM D 790 at a

crosshead speed of 1 mm/min. The flexural modulus and flexural strength were determined. In all cases, the average values of five specimens were taken for each sample.

Impact testing with specimen dimensions of 63.5 × 12.7 × 3.2 mm<sup>3</sup> was done at room temperature (23°C) with a Galdabini 1890 impact pendulum tester [Cardano al Campo (VA), Italy]. The test was carried out according to ASTM D 256, and the energy used was 5.50 J. The unnotched and notched Izod impact strengths were determined from the average values of eight tested specimens.

#### Mode of failure analysis

The mode of fracture was studied by the analysis of the fracture surfaces of the tensile test specimens. This was carried out with a Zeiss Supra 35VP scanning electron microscopy (SEM) machine (Oberkochen, Germany). The fracture surfaces of the tensile test specimens were coated with a thin gold–palladium layer to prevent electrical charge accumulation during the examination.

## RESULTS AND DISCUSSION

### MFI determination

Table III shows the MFI values of the PP, PP/WF, and PP/WF/FR composites. The incorporation of fillers hinders plastic flow and results in an increase in the viscosity of the polymer melt. As a result, there are lower MFI values as the filler content increases. A decrease in the MFI with the incorporation of the WF and FR is expected. The FRs used in this study were in a particulate form that was much smaller in size than the WF (see the Experimental section and Table I). The incorporation of an FR as a replacement for half of the WF could increase the resistance to flow because of the increased amount of contact surface between the particles and matrix, which resulted in the reduction of the viscosity and MFI values of the PP/WF/FR composites. However, with the addition of the MAPP compatibilizer to the filled system, the MFI values were found to slightly increase. Generally, an increase in MFI values indicates better molecular motion of the polymer chains. Possible reasons for this phenomenon include a change in the molecular weight distribution and a lubricating/plasticizing action induced by the coupling agent or compatibilizer.<sup>11</sup> The presence of the silane-treated APP FR (APP2) did significantly change the MFI value of the PP3 composite.

### TGA

Figures 1 and 2 show the TGA and differential thermogravimetry (DTG) curves of PP and its composites. The related TGA data are summarized in Table

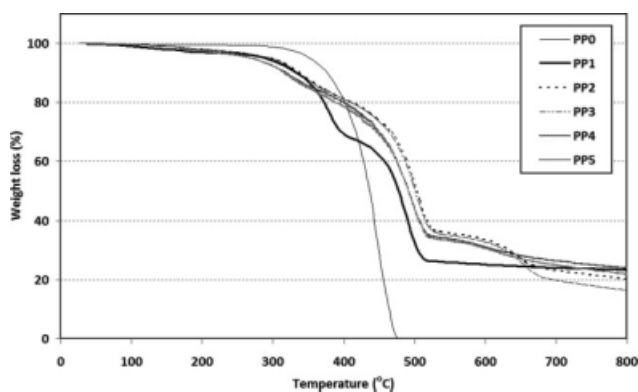


Figure 1 TGA thermograms of PP and its composites.

IV. On the basis of 1% mass loss, PP showed the highest thermal stability because of a very high initial temperature ( $T_{\text{initial}}$ ) of 295°C. The TGA curve of virgin PP (PP0) showed a single mass-loss step with a maximum degradation rate [the first peak degradation rate ( $R_{1\text{peak}}$ )] centered at 448°C [the first peak temperature ( $T_{1\text{peak}}$ )]. At 450°C, the residue content of PP was 29.7 wt %, with nearly no residue content at 485°C.

The incorporation of 60 wt % WF into PP (PP1) reduced  $T_{\text{initial}}$  from 295 to 105°C, probably because of the low thermal stability of WF. This is in agreement with earlier work reported by Li and He.<sup>3</sup> After the initial loss, PP1 exhibited two decomposition steps at 378 ( $T_{1\text{peak}}$ ) and 488°C [the second peak temperature ( $T_{2\text{peak}}$ )], which were related to the decomposition of WF and PP, respectively. The presence of WF increased the thermal decomposition temperature of the PP component from 448 to 488°C. This suggests that WF promoted char formation and thereby delayed the degradation of PP. WF has a component called lignin that acts as a char former, which could reduce the thermal degradation of the PP/WF composites. Lignin is an amorphous polyphenolic plant constituent, and it represents 20–30 wt % of the wood.<sup>12</sup> Lignin can form char during thermal degradation. Char formation is a basic aspect of FR additives because the char reduces the combustion rate of polymeric materials by not allowing the oxygen to easily reach the combustion zone.<sup>13</sup>

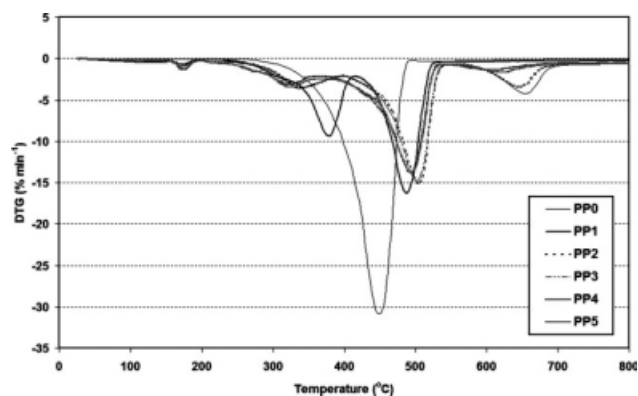


Figure 2 DTG thermograms of PP and its composites.

For the PP2 composite, the incorporation of 30 wt % APP1 FR into the PP/WF system increased the thermal stability ( $T_{\text{initial}}$ ) of the composite from 105 to 141°C. The presence of APP1 enhanced  $T_{2\text{peak}}$  of the PP component from 488°C for PP/WF (PP1) to 505°C for PP/WF/APP1 (PP2). This indicates that APP1 changed the thermal degradation behavior of the PP/WF system and promoted char formation for the composite. There are many chemical reactions involved in fire-protection mechanisms. APP is an effective FR for materials with high oxygen contents, such as cellulose and some oxygen-containing plastics. When plastics or other materials that contain APP are exposed to an accidental fire or heat, the FR starts to decompose, commonly into poly(phosphoric acid) and ammonia. The poly(phosphoric acid) reacts with hydroxyl or other groups of a synergist to form an unstable phosphate ester. In the next step, the dehydration of the phosphate ester follows. A carbon foam is built up on the surface against the heat source (charring). The carbon foam (char) acts as an insulation layer and prevents volatile, combustible gases or further decomposition of the material.<sup>14,15</sup> The char residues of PP1 without an FR were 62.3 wt % at 450°C and 25.1 wt % at 600°C, whereas those of the PP2 system were 74.1 and 33.7 wt %, respectively.

For the PP3 composite, the incorporation of 30 wt % APP2 FR into the PP/WF system led to an increase in the thermal stability of the composite from 105 to 151°C. The thermal stability was slightly

TABLE IV  
Thermal Degradation and Char Residue Data by TGA

Sample code	$T_{\text{initial}}$ (°C)	$R_{1\text{peak}}$ (%/min)/ $T_{1\text{peak}}$ (°C)	$R_{2\text{peak}}$ (%/min)/ $T_{2\text{peak}}$ (°C)	$R_{3\text{peak}}$ (%/min)/ $T_{3\text{peak}}$ (°C)	Char residue (%)	
					450°C	600°C
PP0	295	30.6/448	—	—	29.7	0
PP1	105	7.7/378	15.3/488	—	62.3	25.1
PP2	141	2.1/339	14.0/505	2.6/647	74.1	33.7
PP3	151	2.1/335	13.7/503	3.4/654	73.6	32.8
PP4	148	1.1/325	12.6/494	0.7/609	70.1	31.2
PP5	147	1.3/324	12.4/494	0.8/616	69.1	30.8



TABLE V  
UL94-V and LOI Testing Results for PP and Its Composites

Sample code	UL94-V rating (3.2 mm)	Maximum flaming time for each specimen (s)	Total flaming time for all five specimens (s)	Cotton ignition	LOI (%)
PP0	Not rated	>60	>300	Yes	19
PP1	Not rated	>60	>300	Yes	20
PP2	V-0	5	18	No	23
PP3	V-0	7	20	No	23
PP4	V-0	1	5	No	24
PP5	V-0	1	5	No	24

higher in comparison with that of the PP2 system, probably because of the better dispersion of APP particles in the PP matrix. This was because the APP particles of the APP2 FR were coated with silane, which improved compatibility with the PP matrix. Similar to APP1, APP2 also increased  $T_{2\text{peak}}$  of the PP system from 488°C for PP/WF (PP1) to 503°C for PP/WF/APP2 (PP3). The char residues of the PP2 and PP3 composites were also higher than that of PP1, as can be seen in Table IV.

An improvement in the thermal stability of the PP/WF (PP1) composite could also be observed with the addition of 30 wt % IFR (PP4 and PP5). Both the PP4 and PP5 composites displayed higher thermal stability than PP2. The presence of the IFR also enhanced  $T_{2\text{peak}}$  of both the PP4 and PP5 composites from 488 (PP1) to 494 and 494°C, respectively. This finding demonstrates that the char layer protected the PP composite from decomposing and prolonged the thermal decomposition temperature of the PP component. In comparison with APP1 and APP2, reactions between the three main components (the catalyst, char promoter, and blowing agent) of the IFR led to an expansion process in which a large-volume, high-carbon protective layer developed that effectively protected the underlying substrate from the attack of heat. The large amounts of char residue for both the PP4 and PP5 composites prove that the IFR could promote char formation in the

PP/WF/IFR composites. After decomposition at 600°C, the PP4 and PP5 composites left char residue of about 31.2 and 30.8 wt %, respectively.

### FR properties

Table V shows the UL94-V testing results for PP and its composites. In the absence of an FR, the pure PP (PP0) and the 60 wt % WF-filled PP composite (PP1) burned easily with accompanying melt dripping, which ignited the cotton beneath the burning specimens. This observation indicates the high sensitivity of the pure PP and WF to flame. As the entire samples were consumed during the burning, both the pure PP and PP/WF composite could be classified as not rated according to UL94-V standard specifications.

The presence of 30 wt % APP1 or APP2 in the PP/WF composites enhanced their flame-retardancy properties (the PP2 and PP3 composites). Both the PP2 and PP3 composites were observed to have char formation on the composite surfaces during combustion. The char caused the composites to exhibit flame self-extinguishment, with maximum flaming times of about 5 and 7 s for the PP2 and PP3 composites, respectively, after the flame was removed. No melt dripping was observed from the burning samples of these composites. These characteristics enabled the

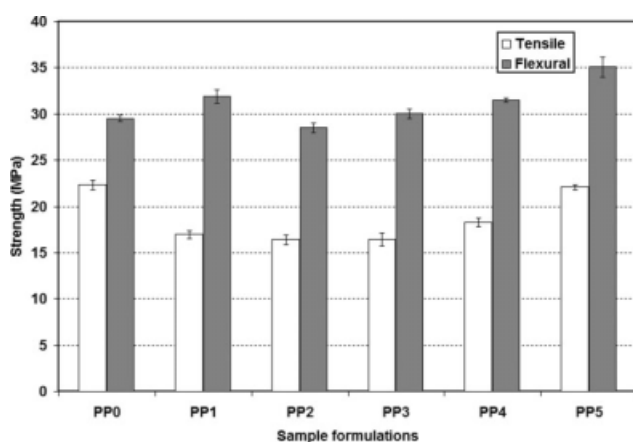


Figure 3 Tensile and flexural strength of PP and its composites.

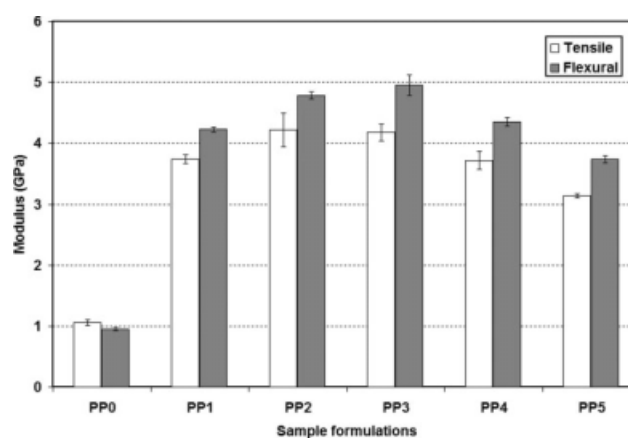
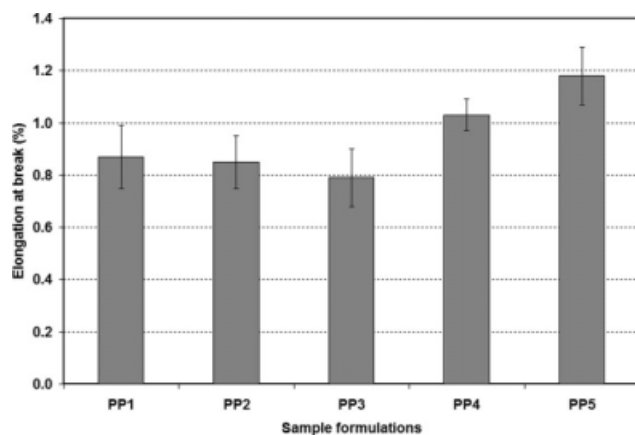


Figure 4 Tensile and flexural modulus of PP and its composites.



**Figure 5** Elongation at break of PP ( $473.6 \pm 51.2\%$  for PP0) and its composites.

PP2 and PP3 composites to achieve a V-0 classification.

The use of a ready-to-use IFR also allowed both the PP4 and PP5 composites to achieve V-0 classification. Compared to the PP2 and PP3 composites, the composites with the IFR showed much lower values of both the maximum and total flaming times (Table V). This was due to the effectiveness of the IFR process, which led to the formation of a large-volume, high-carbon layer for better protection of the composites against the heat source. This observation agrees well with previous studies.<sup>3,9,10</sup>

The LOI test measures the minimum oxygen concentration required to support combustion. The results of the test for the pure PP and all the PP/WF/FR composites are also shown in Table V. The pure PP (PP0) and the PP/WF composite (PP1) showed LOI values of 19 and 20%, respectively. Because normal atmosphere air is approximately 21% oxygen, both PP0 and PP1 are flammable materials. The increase in the LOI value with the incorporation of the APP and IFR indicates that both materials could be considered effective FRs for PP/WF composites.

### Mechanical properties

Figures 3–6 show the mechanical properties of PP and its composites. In the absence of any types of fillers or additives, the pure PP showed the highest tensile strength and elongation at break but the lowest tensile modulus in comparison with the PP composites. The addition of 60 wt % WF (PP1) caused a decrease in the tensile strength, probably because WF is a polar material, whereas the PP matrix is a nonpolar material. As a polar material, WF has a strong tendency to form agglomerates, which result in poor interfacial adhesion between WF and the PP matrix. As the weak region increases, the crack can propagate more easily; this leads to fracture, and

hence the energy to break is reduced.<sup>16</sup> The increase in the modulus is mainly influenced by the incorporation of rigid fiber reinforcements into the polymer. The increase in the tensile and flexural moduli of the PP/WF composite shows the ability of WF to impart greater stiffness to the composite. This result is in agreement with the trend observed for other lignocellulosic-filled thermoplastics.<sup>17–19</sup>

As expected, the addition of rigid, particulate FR additives into PP tended to increase the stiffness but decrease other mechanical properties (e.g., the tensile and flexural strength). All PP/WF/FR composites showed lower tensile strength than pure PP, as shown in Figure 3. This could be attributed to the poor interaction and compatibility of the FR and WF with PP. The deterioration of the mechanical properties of plastics with the addition of FR has been reported by several researchers.<sup>1,5,20,21</sup> A compatibilized PP/WF composite with the IFR (PP5), however, showed a 21% increase in the tensile strength, which was probably due to the improved interaction between WF and the PP matrix in the presence of MAPP. In comparison with PP4, the PP5 composite showed an 11% increase in flexural strength, which was probably due to a better interaction between WF and the PP matrix in the presence of MAPP.

There are many studies concerning the action of MAPP, and most of them have shown a significant improvement (from 25 to 100%) in the mechanical properties of MAPP-treated composites.<sup>22,23</sup> These values vary according to the grafting ratio and the average molar mass of MAPP as well as the processing parameters.<sup>24</sup> MAPP interacts with both the fibers and the matrix and thus creates a link between them. The PP segment of MAPP forms compatible blends with bulk PP through cocrystallization, and the polar part of MAPP (maleic anhydride) forms chemical bonds with the wood.<sup>25</sup> The acidic anhydride groups of MAPP lead to hydrogen

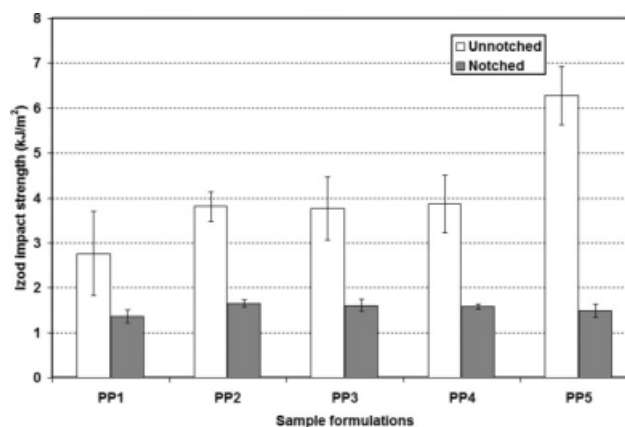


**Figure 6** Izod impact strength of PP (unnotched strength =  $111.33 \pm 1.70$  kJ/m<sup>2</sup> for PP0, notched strength =  $5.81 \pm 0.64$  kJ/m<sup>2</sup> for PP0) and its composites.

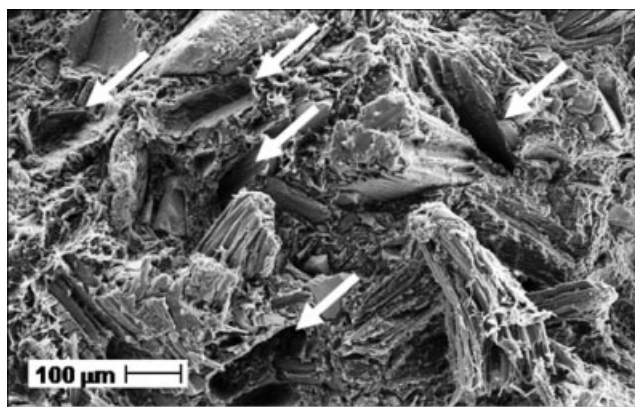


**Figure 7** SEM micrograph of PP1. Voids and cavities are depicted by arrows.

and chemical bonds with the hydroxyl groups of cellulose (esterification reaction), which strongly anchor the reactive groups onto the fiber surface.<sup>26</sup> Furthermore, the PP chains of MAPP smooth the two different surface energies of the matrix and the reinforcement fibers. These aspects help to achieve better wetting of the fibers in the melted polymer, and as a result, the interfacial adhesion is improved.<sup>27,28</sup>

The addition of the WF and FR increased the modulus of PP. The PP2 and PP3 composites showed the highest tensile and flexural moduli among the PP composites. The PP3 composite showed a slight improvement in the flexural strength and modulus in comparison with the PP2 composite. This improvement could be attributed to the use of the silane-treated APP FR, which could improve the dispersion of APP particles in the composites. The relatively lower modulus of the PP4 composites may be attributed to the lower rigidity of the IFR in comparison with APP1 and APP2 (cf. Table I). PP5 showed the lowest tensile and flexural moduli of all the PP composites, probably because of a plasticizing effect contributed by the presence of

MAPP. However, the PP4 and PP5 composites showed more balanced properties as far as strength and stiffness properties are concerned. The incorporation of the WF and FR into PP resulted in a drastic drop in the elongation at break. It appears that the failure mode of the PP matrix shifted from ductile to brittle with the incorporation of both materials. This was expected because the presence of the filler reduced the deformability of the rigid interphase between the filler and the polymer matrix.<sup>19,29</sup>

The unnotched Izod impact strength of the PP/WF composites (in the presence of the IFR, APP, and MAPP) was lower than that of the pure PP, as shown in Figure 6. The incorporation of 60 wt % WF (PP1) reduced the impact strength, and this could be attributed to the nature of the large WF particles. Large particles act as flaws that can easily initiate cracks. According to Griffith's theory, a large aggregate is a weak point that lowers the stress required for the composite to fracture.<sup>30</sup> The replacement of 30 wt % WF with 30 wt % FR resulted in a slight increase in the unnotched Izod impact strength of the PP2, PP3, and PP4 composites. According to Riley et al.,<sup>31</sup> the impact strength depends on both the size and the shape of the filler and is also affected by the micromorphology. The impact strength is enhanced by small, low-aspect-ratio filler particles and a good particle dispersion in the polymer matrix.<sup>31,32</sup> Therefore, the incorporation of a small-particle FR (cf. Table I) could improve the impact strength of PP/WF/FR composites. Among the composites, PP5 had the highest unnotched Izod impact strength. This could be attributed to the improved interfacial adhesion between the PP matrix and the WF in the presence of MAPP.<sup>33</sup> All the composites showed a lower notched Izod impact strength than pure PP. All the composites also showed comparable notched Izod impact strength values.

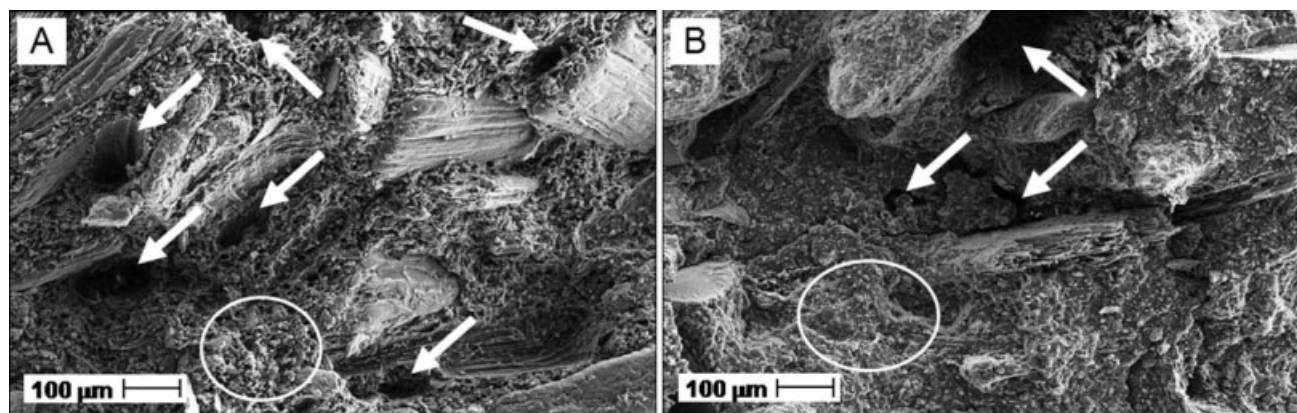


**Figure 8** SEM micrographs of (A) PP2 and (B) PP3. Voids and cavities are depicted by arrows. Circles show (A) poor and (B) improved APP dispersion in the PP matrix.



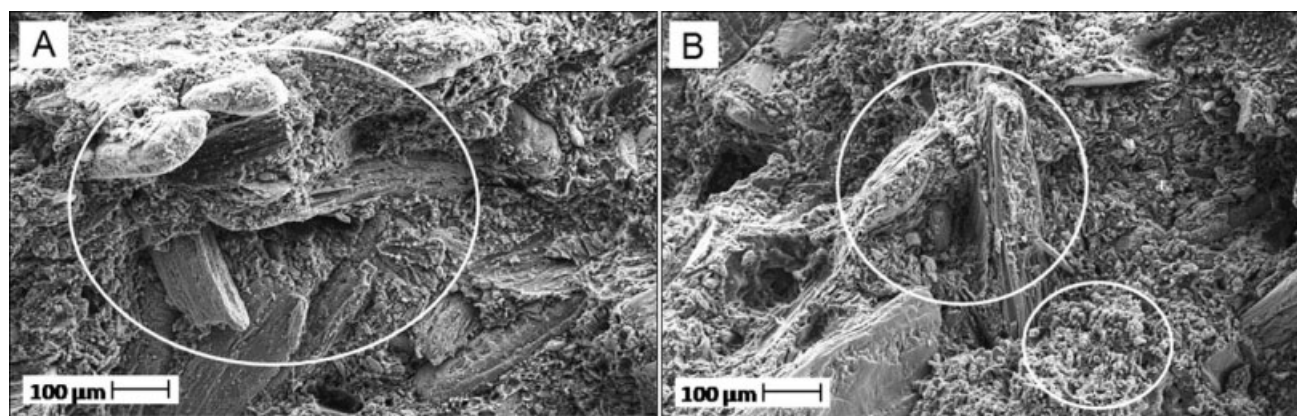


**Figure 9** SEM micrographs of (A) PP4 and (B) PP5. Circles show (A) WF-particle-rich areas and (B) improved wetting of the fillers (WF and FR) by the matrix.

## SEM

Figures 7–9 show SEM micrographs of the PP composites. Figure 7 shows an SEM micrograph of the 60 wt % WF-filled PP composite (PP1). The composite had a rough morphology, with the presence of many voids and cavities resulting from WF pullout. This indicated poor interfacial adhesion between the PP matrix and the WF filler.<sup>34</sup> This then resulted in a detrimental effect on the ultimate performance (the tensile, flexural, and impact strength) of the PP/WF composites.

The PP/WF/FR composite exhibited a brittle failure mode, as shown in Figure 8(A). The WF and FR particles showed poor compatibility with the PP matrix, which resulted in the formation of voids and agglomerations. The WF particles did not seem to be dispersed well around the PP matrix. As a result, the tensile and flexural strength and toughness properties (the elongation at break and impact strength) of the PP/WF/FR composites were reduced. The use of silane-coated APP (APP2) completely changed the morphology of the PP3 composite. In the PP3 composite, the APP particles dispersed more uniformly and displayed a smoother surface in comparison with PP2, as shown in Figure 8(B). This explains the improved flexural strength, flexural modulus, and thermal stability ( $T_{\text{initial}}$ ) of PP3 in comparison with PP2 (cf. Figs. 3 and 4 and Table IV)

The presence of MAPP changed the morphology of the PP5 composite. The SEM micrograph shown in Figure 9(B) proves that the presence of MAPP can improve the wetting of the fillers (WF and FR) by the matrix, which gives rise to strong interfacial adhesion.<sup>18</sup> From the fracture surface, it is clear that the WF particles were heavily coated by the matrix, in contrast to the situation in PP4. This was due to the addition of MAPP, which facilitated the interaction between the WF and PP. This SEM micrograph indicates an increase in adhesion between the WF

and the PP matrix, which was the major reason for the improved strength and toughness properties.

## CONCLUSIONS

The effects of three types of commercial FRs on the flammability and mechanical properties of PP/WF composites were studied. The incorporation of an FR into the PP/WF composites led to a remarkable effect on the charring and thermal stability of the PP formulations, as revealed by TGA. It was evident that pure PP and the PP/WF composite displayed poor FR properties. The incorporation of FR reduced the flammability and increased the LOI of PP/WF, and thus V-0 UL94 classification was achieved. The flame-retardancy behavior of PP/WF was further enhanced with the incorporation of the IFR because of the synergistic effects of their constituent materials. The incorporation of the rigid FR into PP/WF led to a significant enhancement of the stiffness. However, this enhancement was accompanied by a reduction in the tensile, flexural, and Izod impact strength and the elongation at break. Further improvement of the mechanical properties, especially the strength properties, was achieved via the incorporation of MAPP. This was attributed to the improvement of the filler–matrix adhesion between the WF and the PP matrix.

## References

- Sain, M.; Park, S. H.; Suhara, F.; Law, S. *Polym Degrad Stab* 2004, 83, 363.
- Chen, Y.; Liu, Y.; Wang, Q.; Yin, H.; Aelmans, N.; Kierkels, R. *Polym Degrad Stab* 2003, 81, 215.
- Li, B.; He, J. M. *Polym Degrad Stab* 2004, 83, 241.
- Atikler, U.; Demir, H.; Tokati, F.; Tihminlioglu, F.; Balkose, D.; Ulku, S. *Polym Degrad Stab* 2006, 91, 1563.
- Li, B.; Xu, M. *Polym Degrad Stab* 2006, 91, 1380.
- Suarez, J. C. M.; Coutinho, F. M. B.; Sydenstricker, T. H. *Polym Test* 2003, 22, 819.
- Zhang, S.; Horrocks, A. R. *Prog Polym Sci* 2003, 28, 1517.



8. Abu Bakar, M. B.; Mohd Ishak, Z. A.; Mat Taib, R.; Rozman, H. D.; Mohamad Jani, S. *Proc Pacific Rim Bio-Based Compos Symp* 2006, 8, 349.
9. Le Bras, M.; Duquesne, S.; Fois, M.; Grisel, M.; Poutch, F. *Polym Degrad Stab* 2005, 88, 80.
10. Anna, P.; Marosi, G.; Bourbigot, S.; Le Bras, M.; Delobel, R. *Polym Degrad Stab* 2002, 77, 243.
11. Ai Wah, C.; Leong, Y. C.; Gan, S. N. *Eur Polym J* 2000, 36, 789.
12. De Chirico, A.; Armanini, M.; Chini, P.; Cioccolo, G.; Provasoli, F.; Audisio, G. *Polym Degrad Stab* 2003, 79, 139.
13. Pearce, C. E.; Khanna, Y. P.; Raucher, D. In *Thermal Characterization of Polymeric Materials*; Tiri, E. A., Ed.; Academic: Orlando, FL, 1981; Chapter 8, p 793.
14. SpecialChem Ammonium Polyphosphate Center. Mechanism of Action. <http://www.specialchem4polymers.com/tc/ammonium-polyphosphate/index.aspx?id=mechanism> (accessed Aug 2008).
15. Pin, L. V. P.; Wang, Z.; Hu, K.; Fan, W. *Polym Degrad Stab* 2005, 90, 523.
16. Ismail, H.; Hong, H. B.; Ping, C. Y.; Abdul Khalil, H. P. S. *J Thermoplast Compos Mater* 2003, 16, 121.
17. Van De Velde, K.; Kiekens, P. *J Thermoplast Compos Mater* 2002, 15, 281.
18. Rozman, H. D.; Kon, B. K.; Abu Samah, A.; Kumar, R. N.; Mohd Ishak, Z. A. *J Appl Polym Sci* 1998, 69, 1993.
19. Zaini, M. J.; Fuad, M. Y. A.; Ismail, Z.; Mansor, M. S.; Mustafah, J. *Polym Int* 1996, 40, 51.
20. Almeras, X.; Le Bras, M.; Hornsby, P.; Bourbigot, S.; Marosi, G.; Keszie, S.; Poutch, F. *Polym Degrad Stab* 2003, 82, 325.
21. Nachtigall, S. M. B.; Miotto, M.; Schneider, E. E.; Mauler, R. S.; Forte, M. M. C. *Eur Polym J* 2006, 42, 990.
22. Felix, J. M.; Gatenholm, P. *J Appl Polym Sci* 1991, 42, 609.
23. Sanadi, A. R.; Young, R. A.; Clemons, C.; Rowell, R. M. *J Reinforced Plast Compos* 1994, 13, 54.
24. Woodhams, R. T.; Thomas, G.; Rodgers, D. K. *Polym Eng Sci* 1984, 24, 1166.
25. Yuan, X.; Zhang, Y.; Zhang, X. *J Appl Polym Sci* 1999, 71, 333.
26. Cantero, G.; Arbelaiz, A.; Mugika, F.; Valea, A.; Mondragon, I. *J Reinforced Plast Compos* 2003, 22, 37.
27. Bledzki, A. K.; Gassan, J. *Prog Polym Sci* 1999, 24, 221.
28. Boll, D. J.; Bascom, W. D.; Motiee, B. *Compos Sci Technol* 1985, 24, 253.
29. Abu Bakar, M. B.; Leong, Y. W.; Ariffin, A.; Mohd Ishak, Z. A. *J Appl Polym Sci* 2007, 104, 434.
30. Mareri, P.; Bastide, S.; Binda, N.; Crespy, A. *Compos Sci Technol* 1998, 58, 747.
31. Riley, A. M.; Paynter, C. D.; McGenity, P. M.; Adams, J. M. *Plast Rubber Process Appl* 1990, 14, 85.
32. Da Silva, A. L. N.; Rocha, M. C. G.; Moraes, M. A. R.; Valente, C. A. R.; Coutinho, F. M. B. *Polym Test* 2002, 21, 57.
33. Bengtsson, M.; Le Baillif, M.; Oksman, K. *Compos A* 2007, 38, 1922.
34. Nachtigall, S. M. B.; Cerveira, G. S.; Rosa, S. M. L. *Polym Test* 2007, 26, 619.